An Analysis of Ferrite Magnet Assisted Synchronous Reluctance Machines for Low Power Drives including Flux Weakening

Matthias Hofer, Manfred Schrödl
Institute of Energy Systems and Electrical Drives
Technische Universität Wien
Vienna, Austria
matthias.hofer@tuwien.ac.at

***Abstract*—In this paper permanent magnet assisted synchronous reluctance machines are investigated for low power industrial drives. Several drive applications require a constant power demand over a wide speed range up to high rotational speeds. Therefore, electrical drives are usually operated in the flux weakening range. In addition, a high efficiency, a high power factor, low product as well as low operational costs are reasonable demands for future electrical drives. The proposed machine type without rare earth material is a potential candidate for such requirements. The level of pre-magnetization at permanent magnet assisted synchronous machines is not only the key parameter to reach high torque densities, but also mainly responsible to adjust the machine power and the power factor in the flux weakening region. By finite element analysis the V-shape and straight magnet arrangement type rotors with three flux barriers are discussed. Different types of ferrites and the amount of magnets are varied to show the influence on the machine parameters and performance. Further, for a sufficient operation at high speeds a mechanical stress analysis is included. The anti-demagnetization behavior is discussed and results in a limitation of the V-shape topology.**

***Index Terms*—Synchronous Reluctance Machine, Permanent Magnet Synchronous Machine, Industrial Drive**

I. Introduction

In the last years alternative electric machine topologies are discussed intensively for several applications. The reasons are the limited resources and high costs of rare earth permanent magnets usually used in the permanent magnet synchronous machine (PMSM) premium segment. Further, latest efficiency demands for variable speed drives according to IEC 60034-30-2 can not be easily reached by conventional squirrel cage induction machines (IMs). Therefore, synchronous reluctance machines (SynRMs) and Permanent Magnet assisted SynRM (PMaSynRM) are proposed to solve these issues. According to [1], SynRMs may replace IMs by a higher efficiency at same machine size. But for electric drives operated in a wide speed range including flux weakening (FW) the SynRMs provide a poor performance by a massive decrease of torque and power above the nominal speed [2], [3]. A SynRM approach with salient poles is an alternative to flux barriers to improve the part load efficiency [3], but the constant power speed range (CPSR) is still limited. Further, the lower power factor of SynRMs compared to PMSMs requires a higher current rating of the drive inverter. These functional disadvantages of the SynRMs can be solved by assistance of permanent magnets (PMs). Even low energy magnets can improve the machine characteristics significantly. Thus, PMaSynRMs are also proposed for electric vehicles in [4], [5], [6], [7]. For industrial drives, a PMaSynRM with ferrite magnets is able to reach efficiency class IE5 [8] in the same size of an IE2 class IM. Most analysis of PMaSynRMs are related to the torque and efficiency optimization in the base speed range, e.g. [9], [10], but here the focus is set to the high speed operation at FW. In this work an industrial low power application, which currently utilizes an IM-drive, shall be improved by a PMaSynRM, because SynRMs are already analyzed in [3] with a limitation in the FW range. The investigation is focused only on the rotor design of a 24 slot IM stator. For demonstration of the machine behavior at high speeds and evaluation of possible future applications simulations are performed at much higher speeds than the requirements stated in Tab. I.

TABLE I
Drive requirements

Shaft Torque	$\geq$0.6Nm
Shaft Power	$\geq$50W
Operational Shaft Speed	6.000rpm
Number of poles	4
Phase Current	$\leq$0.86A_{RMS}
Line to Line Voltage	$\leq$280V_{RMS}

II. Permanent Magnet Assisted Synchronous Reluctance Machines Description

For the mathematical description of the PMaSynRM the following equations are used. The flux linkage of the permanent magnet Ψ_M is aligned in negative q-axis direction. This is different to the conventional nomenclature of PMSMs, where the permanent flux is aligned in positive d-axis direction. Thus, the flux linkage equations are given as

$$\begin{aligned} \Psi_d &= L_d \; I_d \\ \Psi_q &= L_q \; I_q - \Psi_M \,, \end{aligned} \qquad (1)$$

where I_d is the d-axis current and I_q is the q-axis current respectively. The currents are $I_d = |\underline{I}_{S,dq}| \cos(\beta)$ and $I_q = |\underline{I}_{S,dq}| \sin(\beta)$, where the angle β represents the angular position of the stator current phasor $\underline{I}_{S,dq}$ in the dq-reference frame. The total machine torque M is described as

$$\begin{aligned} M &= \tfrac{3}{2} p \{\Psi_q \; I_d - \Psi_d \; I_q\} \\ &= \tfrac{3}{2} p \{\Psi_M \; I_d + (L_d - L_q) \; I_d \; I_q\} \; , \end{aligned} \tag{2}$$

where the p is the number of pole pairs. The total torque M consists of two parts. First, the permanent magnet torque proportional to $\Psi_M \; I_d$ and second, the reluctance torque which is defined by the inductance difference $L_d - L_q$ and both current components I_d and I_q, see also Fig. 2. Generally, the incutances L_d and L_q strongly depend on the current load, as later will be shown. The PMaSynRM without any permanent magnetization ($\Psi_M = 0$) results in a SynRM machine with maximum torque at $\beta = 45°$. Depending on the PM flux an additional torque component is added and the maximum achievable torque increases. Finally, for the V-shape design in Fig. 1 without the intermediate rib a maximum torque of $M = 1.14$ Nm at $\beta = 35°$ is reached. Note that the influence of the intermediate rib would reduce the maximum torque to $M = 1.06$ Nm at $\beta = 37°$ at nominal current. In several works like [11], [12] optimization strategies and topologies for a maximum torque are investigated. Generally, for PMaSynRMs the machine torque increases significantly compared to the SynRMs, here only approximately the half torque $M = 0.61$ Nm is reached without magnets (see Fig. 3). Further, the efficiency increases at a higher PM flux as shown in [13]. The following sections present analysis results of two different rotor types, a V-shape and a straight magnet topology with different ferrite grades.

III. PMASYNRM DESIGNS

A typical PMaSynRM consists of several flux barrier layers, which can be utilized with PMs. For easy magnet manufacturing and rotor assembly only rectangular brick magnets are considered. In literature also circular or elliptic shapes are known [14], [15].

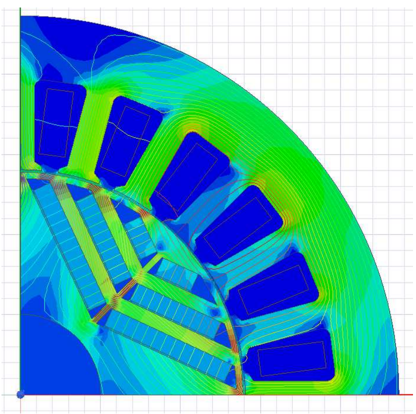

Fig. 1. Four pole V-shape PMaSynRM (section) with three magnet layers and intermediate bridge.

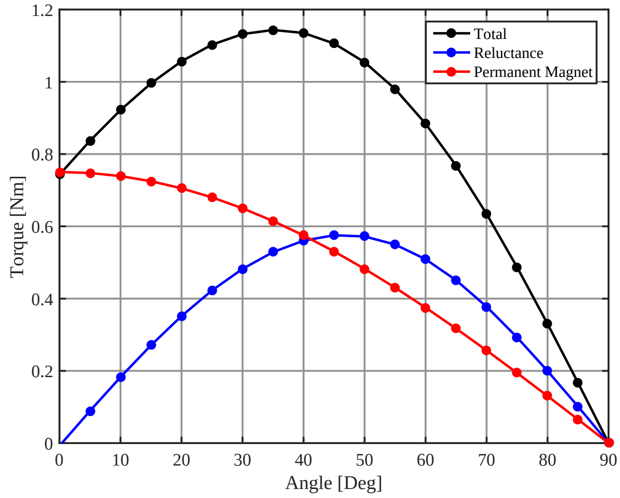

Fig. 2. Torque vs. angle β of three layer V-shape magnets type 24xY30BH without intermediate rib at nominal current.

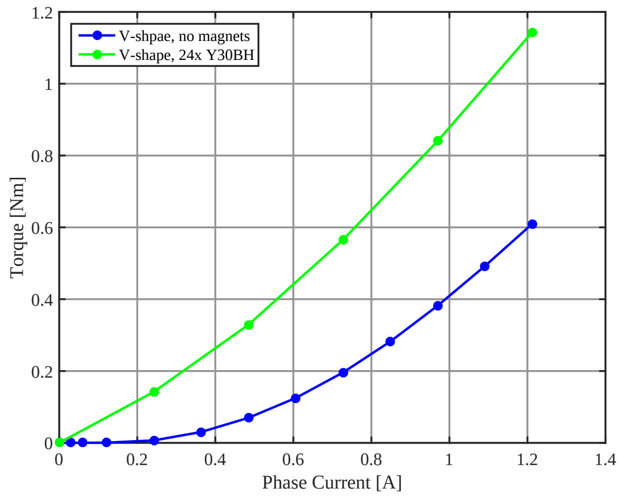

Fig. 3. Torque vs. current characteristic at MTPA, V-shape arrangements without intermediate rib, without and with ferrites 24xY30BH.

A. V-shape arrangement

In Fig. 1 a three layer topology with V-shape arrangement of the magnets is shown. Usually, an intermediate bridge between the magnets is applied to ensure mechanical strength at high speeds. From a magnetic point of view this bridge should be avoided to reduce the PM leakage path. As later is shown, in this application the mechanical strength is sufficient even without an intermediate rib. Now, three different magnetization levels of the V-shape rotor are investigated. Without any magnets (pure SynRM) a low torque vs. current ratio is reached (Fig. 3). A high level pre-magnetization with 24xY30BH magnets ($B_{Rem} = 0.39$T) and a medium magnetization with 24xY10T ($B_{Rem} = 0.2$T) are applied. The pictures Fig. 4 and

Fig. 5 present the flux linkages Ψ_d and Ψ_q and the inductances L_d and L_q respectively. Only a small cross-coupling of the d- and q- axis flux can be seen. Without any PMs the

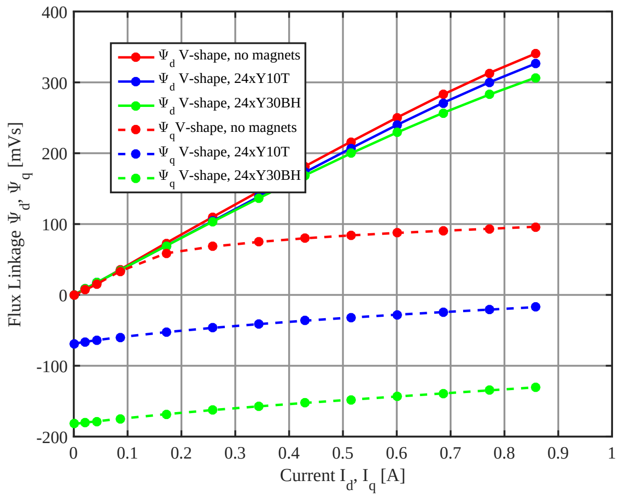

Fig. 4. Flux linkages of V-shape rotor without and with ferrites Y10T and Y30BH.

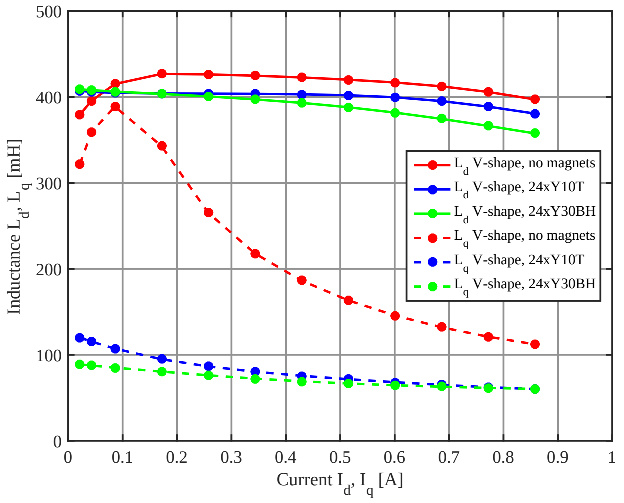

Fig. 5. Inductances of V-shape rotor without and with ferrites Y10T and Y30BH.

inductance ratio varies in a wide range $L_d/L_q \approx 1 - 3.5$ and is quite low because the bridges need to be saturated by $I_q > 0.1$A. By the PM assistance with Y30BH ferrites the ratio $L_d/L_q \approx 4.6 - 5.9$ is significantly higher. Here, the PMs ensure rib saturation already at zero current and the inductance L_q stays always low, see Fig. 5. Consequently, each setup has a different PM flux Ψ_M (Tab. II) and these differences lead to various torque and power characteristics over the speed range depicted in Fig. 6 and Fig. 7. As expected with higher pre-magnetization, both an increase of maximum torque at low speeds as well as an increased power capability in FW can be gained compared to the pure SynRM, although this topology without the intermediate bridge already fulfills the requirements. Depending on the operation range, the maximum torque per ampere (MTPA) strategy is applied at low speeds and at limited stator voltage in FW operation the MTPV (maximum torque per volt) approach is implemented. The medium magnetization shows a wide CPSR, but a very high level of magnetization leads to a poor power and even a limited speed at 12.500rpm. This confirms the recommendation of carefully designing the PM volume or magnets B_{Rem} related to high operational speeds [13] and choice of the machine's characteristic current [7].

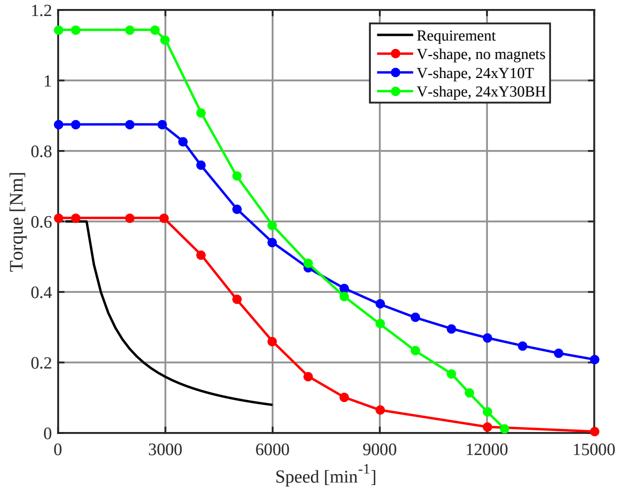

Fig. 6. Torque vs. speed characteristic, V-shape arrangements without and with ferrites Y10T and Y30BH.

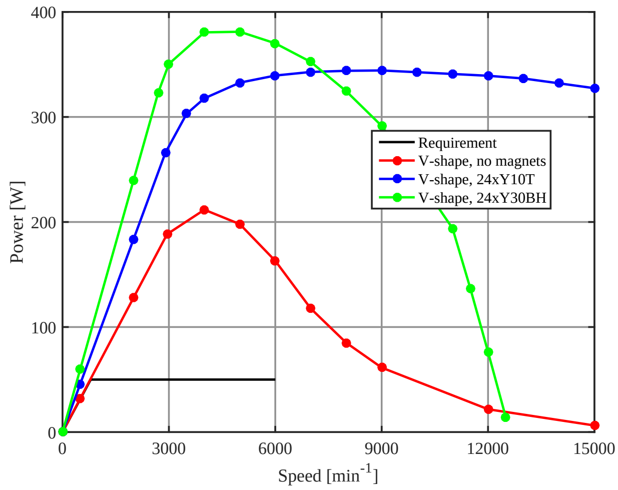

Fig. 7. Power vs. speed characteristic, V-shape arrangements without and with ferrites Y10T and Y30BH.

B. Straight Magnet Arrangement

Contrary to the V-shape topology, at the straight magnet arrangement only one magnet per layer and pole is used according to Fig. 8. Thus, the number of magnets is reduced from 24 to 12 which decreases the manufacturing and assembly

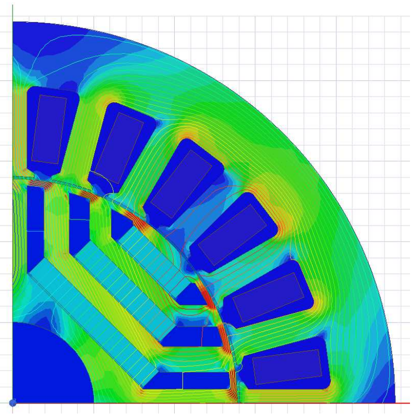

Fig. 8. Straight PMaSynRM with three layer magnets.

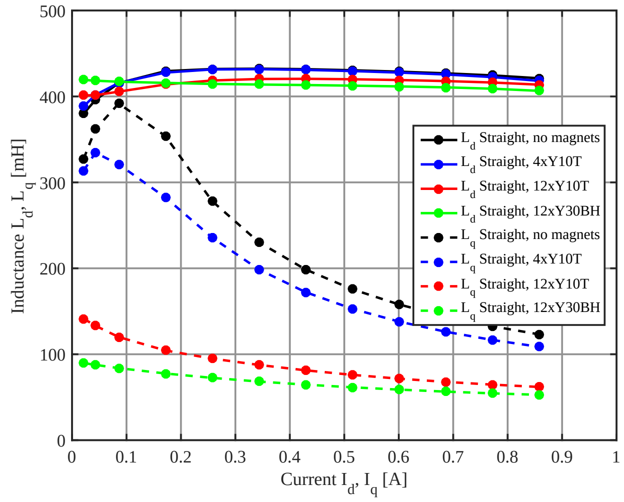

Fig. 10. Inductances of the PMaSynRMs with straight magnets, ferrite types Y10T and Y30BH.

effort in rotor production. Fig. 9 shows the flux linkages in d- and q-direction related to the magnetization level. Again, the flux linkage Ψ_d is nearly independent from the permanent magnet flux Ψ_M. In contrast to a high magnetization state, at a very low PM flux using only one magnet layer the total flux linkage Ψ_q nearly always has a positive sign and the PM flux is only $\Psi_M = 1\text{mVs}$, see Tab. II. But this already affects the machine inductances as shown in Fig. 10 and the saliency ratio $L_d/L_q \approx 1.2 - 3.9$ is slightly improved compared to SynRMs. By utilization of just the outer four magnets (4xY10T) the machine torque is increased to 0.66Nm (compare V-shape type, no magnets in Fig. 6) but high speed behavior is quite similar to SynRMs. As expected, according to Fig. 11 the maximum torque in low speed range increases with higher flux Ψ_M, see Tab. II . Additionally, the PM flux Ψ_M strongly affects the performance in the high speed range. The PMaSynRM output power variation with straight magnets in MTPV operation is depicted in Fig. 12. A very small CPSR is given for the single magnet (blue) and the power decreases dramatically at higher speeds similar to pure SynRMs. With three magnet layers (low B_{Rem}) the CPSR range is enlarged (red). At a high pre-magnetization level (green) a nearly constant output power of 380W is reached at increasing speed. This graphic clearly demonstrates the high impact of the pre-magnetization level on PMaSynRMs also at high speeds.

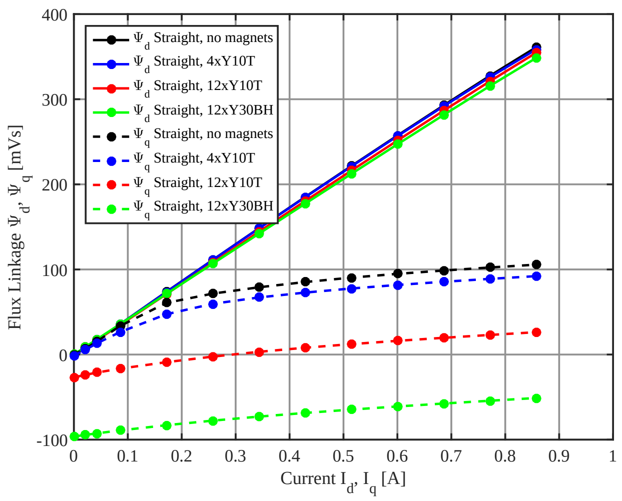

Fig. 9. Flux linkages of the PMaSynRMs with straight magnets, ferrite types Y10T and Y30BH.

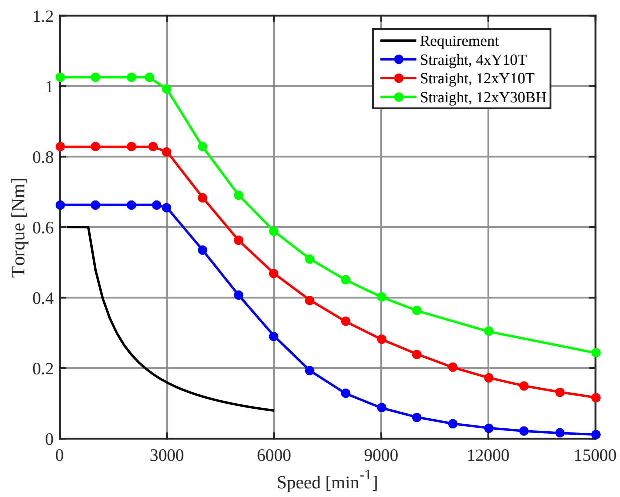

Fig. 11. Torque characteristic of the PMaSynRMs with straight magnets, ferrite types Y10T and Y30BH.

IV. Comparison

To compare both rotor topologies the torque and power performance, as well as machine parameters are used. Further, the mechanical robustness and anti-demagnetization capability are discussed.

A. Torque and power performance

The pre-magnetization level is a key parameter in PMaSynRM design. With increasing PM-flux Ψ_M the param-

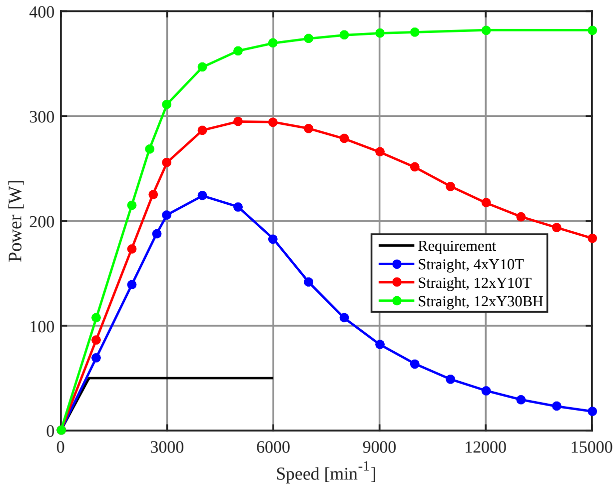

Fig. 12. Power characteristic of the PMaSynRMs with straight magnets, ferrite types Y10T and Y30BH.

eters (Tab. II) show a wide variance from a SynRM up to a PMSM behavior. The V-shape with highest magnetization 24xY30BH has the highest flux linkage 182mVs which consequently leads to a very high Back-EMF voltage $U_{LL,peak} = 981V$ at 15.000rpm and is nearly three times higher than the nominal line-to line peak voltage 396V. Further, this rotor shows the highest characteristic current or short circuit current for infinite speed $I_{S,SC} = \Psi_M/L_q$=3.03A. These parameters lead to a limited performance in FW range. The saliency ratio is $L_d/L_q \approx 4.6 - 5.9$. The straight topology with 12xY30BH provides the highest saliency ratio $L_d/L_q \approx 4.6 - 7.7$, although the flux linkage yields only 96.3mWb. This is caused by the total magnet volume. The V-shape utilizes a magnet mass of 181.5g (volume 37.4cm^3) and the straight arrangement has only 151.6g (volume 31.2cm^3). This is a reduction of 16% and half number of magnets compared to the V-shape type. With a lower characteristic current $I_{S,SC} = 1.85A$ an infinite CPSR can be reached (Fig. 6), although the maximum torque is only 1.02Nm. Finally, all PM assisted approaches presented in this work easily fulfill the given drive requirements, but with an appropriate design, significant higher torques and even up to seven times higher power than required can be realized with a PMaSynRM topology.

TABLE II
PM FLUX LINKAGE

Arrangement	Flux linkage Ψ_M	Inductance L_q	Current $I_{S,SC}$	Voltage $U_{LL,peak}$
straight 4xY10T	1mVs	108mH	≈0	5V
straight 12xY10T	26.9mVs	62mH	0.43A	145V
straight 12xY30BH	96.3mVs	52mH	1.85A	518V
V-shape 24xY10T	68.8mVs	60mH	1.15A	371V
V-shape 24xY30BH	182mVs	60mH	3.03A	981V

B. Mechanical stress

For flux barrier SynRMs and PMaSynRMs the mechanical stress in ribs and bridges is a key design parameter. They should be as thin as possible for a low leakage flux within the rotor but also withstand mechanical stress during nominal and overload conditions. The minimal thickness often is limited by the manufacturing process. For both designs the circumferential rib is 0.8mm. The analysis of the V-shape rotor according to Fig. 13 shows a possible operation within linear material range up to a speed of 18.500rpm. At the straight arrangement (Fig. 14) the linearity is given up to 16.000rpm. A significant plastic deformation occurs above 23.700rpm for both topologies. Thus, both rotor types ensure operation up to intended speed of 16.000rpm and show potential reduction of the rib thickness for lower operational speeds.

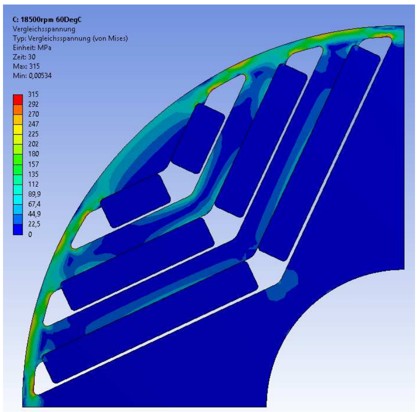

Fig. 13. Mechanical equivalent stress (von Mises) of V-shape rotor with ferrites at 18.500rpm.

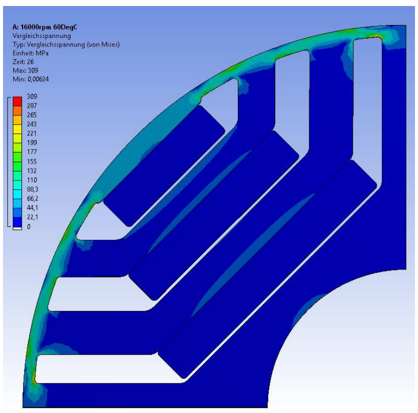

Fig. 14. Mechanical equivalent stress (von Mises) of straight rotor with ferrites at 16.000rpm.

C. Demagnetization

During an optimal operation of the PMaSynRM a high reverse flux to the PM is applied by the flux component $L_q I_q$ and the total flux linkage Ψ_q even may change its sign according to Fig. 9. Thus, demagnetization of the ferrites is a major issue in the PMaSynRM design [14], [15], [16]. The investigation is based on the magnet's BH-curve, as depicted in Fig. 15. Irreversible demagnetization occurs for magnetic load points leaving the linear range of the BH-curve. The low B_R ferrite Y10T shows linear behavior in the whole range for $B \geq 0$, but with Y30BH the flux density should be always $B \geq 0.22T$. Definitely, the BH-curve changes over temperature and as also shown in [11], [14] the low temperatures at ferrites are more critical for demagnetization than higher temperature levels because of the coercivity's positive temperature coefficient. The minimum PM flux densities according to Tab. III for several stationary load conditions are marked in Fig. 15. The lowest B_{min} at the higher magnetization level (magnet Y30BH) is the short circuit state. The Y10T variants have the lowest B_{min} already at normal operation and short circuit seems not critical. In all cases the no load condition (idle) shows the highest B_{min}. Further, the V-shape topology (red) uses a much wider magnetization range than the straight (blue) topologies. The single layer magnet is not considered. For further analysis the transient load change (sudden short circuit) will be investigated in future work.

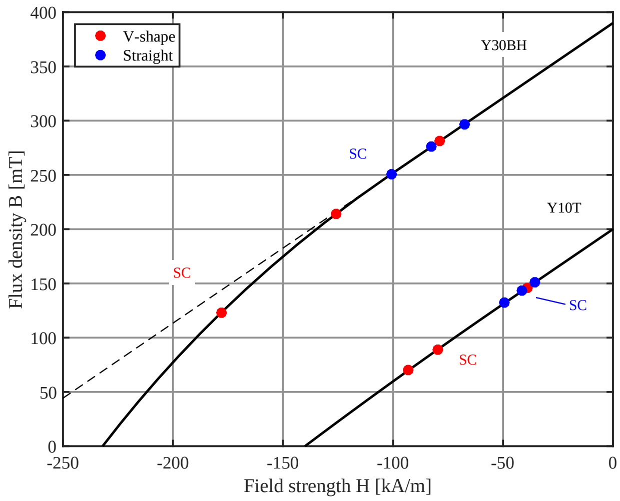

Fig. 15. BH-characteristic of ferrites Y10T and Y30BH with operation points (normal, idle, short circuit) for both rotor topologies V-shape (red) and straight (blue).

TABLE III
MINIMUM PM FLUX DENSITY AND BACK-EMF VOLTAGE

	$B_{min,norm}$	$B_{min,SC}$	$B_{min,idle}$
straight 12xY10T	132mT	143mT	151mT
straight 12xY30BH	276mT	251mT	297mT
V-shape 24xY10T	70mT	89mT	146mT
V-shape 24xY30BH	214mT	123mT	281mT

V. CONCLUSION

This analysis of ferrite magnet assisted SynRMs clearly shows the advantages of higher torque and power compared to pure SynRMs. The comparison of two rotor topologies results in a preference of the straight magnet topology, because it combines a high torque and a wide constant power speed range up to high rotational speeds. Further, the straight arrangement requires only a lower number of magnets and a lower amount of ferrite material. Even the demagnetization analysis has shown a higher robustness against demagnetization of the straight topology. Therefore, based on this investigation, in the next step a prototype with the three layer straight arrangement will be built and experimental tests are planned accordingly.

REFERENCES

[1] A. de Almeida, F. Ferreira, and G. Baoming, "Beyond induction motorstechnology trends to move up efficiency," in *IEEE Transactions on Industry Applications,vol. 50, no. 3,*, May/June 2014.
[2] G. Pellegrino, T. M. Jahns, N. Bianchi, W. Soong, and F. Cupertino, "The rediscovery of synchronous reluctance and ferrite permanent magnet motors," in *SpringerBriefs in Electrical and Computer Engineering*, 2016.
[3] M. Hofer, M. Nikowitz, and M. Schrödl, "Power and efficiency of salient pole and flux barrier type synchronous reluctance machines in low power drives," in *EPE'2018, ECCE Europe*, 2017.
[4] K. S. Khan, "Design of a permanent-magnet assisted synchronous reluctance machine for a plug-in hybrid electric vehicle," in *Licentiate Thesis, KTH Royal Institute of Technology*, 2011.
[5] P. Li, W. Ding, and G. Liu, "Sensitivity analysis and design of a high performance permanent-magnet-assisted synchronous reluctance motor for ev application," in *IEEE Transportation Electrification Conference and Expo (ITEC)*, 2018.
[6] H. Cai, B. B. Guan, and L. Xu, "Low-cost ferrite pm-assisted synchronous reluctance machine for electric vehicles," in *IEEE Transactions on Industrial Electronics*, vol. 61, 2014, pp. 5741 – 5748.
[7] T. Huynh and M. Hsieh, "Comparative study of pm-assisted synrm and ipmsm on constant power speed range for ev applications," in *IEEE Transactions on Magnetics*, vol. 53, 2017.
[8] V. Prakht, V. Dmitrievskii, and V. Kazakbaev, "Mathematical modeling ultra premium efficiency (ie5 class) pm assisted synchronous reluctance motor with ferrite magnets," in *25th International Workshop on Electric Drives: Optimization in Control of Electric Drives (IWED)*, 2018.
[9] T. Mohanarajah, M. Nagrial, J. Rizk, and A. Hellany, "Permanent magnet optimization in pm assisted synchronous reluctance machines," in *IEEE 27th International Symposium on Industrial Electronics (ISIE)*, 2018.
[10] B. Kerdsup, N. Takorabet, and B. Nahidmobarakeh, "Design of permanent magnet-assisted synchronous reluctance motors with maximum efficiency-power factor and torque per cost," in *XIII International Conference on Electrical Machines (ICEM)*, 2018.
[11] M. Barcaro and N. Bianchi, "Interior pm machines using ferrite to replace rare-earth surface pm machines," in *IEEE Transactions on Industry Applications*, vol. 50, 2014, pp. 979 – 985.
[12] N. Bianchi, E. Fornasiero, and W. Soong, "Selection of pm flux linkage for maximum low-speed torque rating in a pm-assisted synchronous reluctance machine," in *IEEE Transactions on Industry Applications*, vol. 51, 2015, pp. 3600 – 3608.
[13] M. Barcaro, N. Bianchi, and F. Magnussen, "Permanent-magnet optimization in permanent-magnet-assisted synchronous reluctance motor for a wide constant-power speed range," in *Transactions on Industrial Electronics*, vol. 59, 2012, pp. 2495 – 2502.
[14] A. Vagati, B. Boazzo, P. Guglielmi, and G. Pellegrino, "Design of ferrite-assisted synchronous reluctance machines robust toward demagnetization," in *IEEE Transactions on Industry Applications*, vol. 50, 2014, p. 17681779.
[15] H. Huang, Y.-S. Hu, Y. Xiao, and H. Lyu, "Research of parameters and antidemagnetization of rare-earth-less permanent magnet-assisted synchronous reluctance motor," in *IEEE Transactions on Magnetics*, vol. 51, 2015.
[16] Y. Kong, M. Lin, M. Yin, and L. Hao, "Rotor structure on reducing demagnetization of magnet and torque ripple in a pma-synrm with ferrite permanent magnet," in *IEEE Transactions on Magnetics*, vol. 54, 2018.